A Compact Tri-Band Monopole Antenna With Single-Cell Metamaterial Loading

Jiang Zhu, *Student Member, IEEE*, Marco A. Antoniades, *Member, IEEE*, and George V. Eleftheriades, *Fellow, IEEE*

***Abstract*—A compact tri-band planar monopole antenna is proposed that employs reactive loading and a "defected" ground-plane structure. The reactive loading of the monopole is inspired by transmission-line based metamaterials (TL-MTM), which enables the loaded antenna to operate in two modes. The first resonance exhibits a dipolar mode over the lower WiFi band of 2.40 GHz – 2.48 GHz, and the second resonance has a monopolar mode over the 5.15–5.80 GHz upper WiFi band. Full-wave analysis shows that the currents of the two modes are orthogonal to each other, resulting in orthogonal radiation patterns in the far field. The feature of a "defected" ground-plane, formed by appropriately cutting an L-shaped slot out of one of the CPW ground-planes, leads to the third resonance that covers the WiMAX band at 3.30–3.80 GHz. Air bridges at the intersection between the antenna and the CPW feedline ensure a balanced current. A fabricated prototype has compact dimensions of 20.0 mm × 23.5 mm × 1.59 mm, and exhibits good agreement between the measured and simulated S parameters and radiation patterns. The measured radiation efficiencies are 67.4% at 2.45 GHz, 86.3% at 3.50 GHz and 85.3% at 5.50 GHz.**

***Index Terms*—Defected ground plane, folded monopole antenna, metamaterials, multiband antenna.**

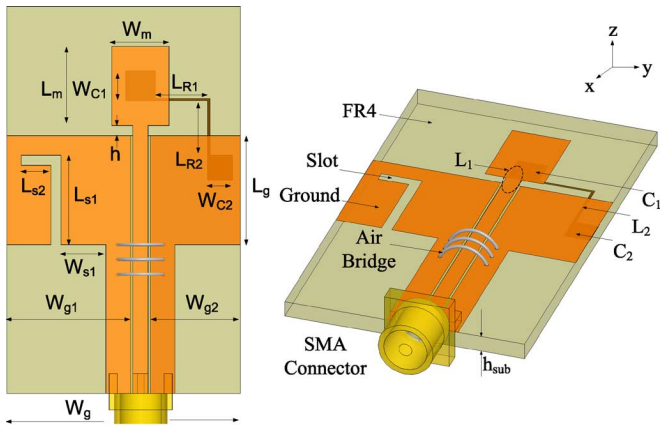

Fig. 1. Tri-band monopole antenna with single-cell MTM loading and a "defected" ground-plane. All dimensions are in mm: $L_m = 8, W_m = 5.8, L_g = 11, W_g = 23.5, W_{g1} = 9.0, W_{g2} = 12.5, h = 1, W_{C1} = 3, W_{C2} = 2.5, L_{R1} = 5.5, L_{R2} = 5.5, L_{s1} = 9, L_{s2} = 3, W_{s1} = 7, h_{sub} = 1.59$ and slot width $g = 1$. (a) Top view. (b) 3D schematic.

I. Introduction

TWO commonly used protocols for Wireless Local Area Networks (WLANs) based on access points to relay data, are WiFi and WiMAX, which promise higher data rates and increased reliability. A challenge in designing such multiple wireless communication protocol systems is to design compact, low cost, multiband and broadband antennas.

The planar monopole is attractive for WLAN antenna design because it has a low profile, it can be etched on a single substrate and can provide the feature of broadband or multiband operation. The traditional approach is to use multibranched strips in order to achieve multiband operation [1], which generally leads to a large volume or requires a large ground-plane. Alternatively, the concept of the frequency-reconfigurable multiband antenna [2] has been proposed to develop multiband monopole antennas for WiFi and WiMAX applications [3]. Such reconfigurable antennas are reported to have the advantages of being able to switch to a desired service and to achieve good out-of band noise rejection performance. However, this is traded off with an increased design complexity and an increased fabrication cost associated with switches and bias circuits.

Transmission-line metamaterials (TL-MTM) [4]–[6] provide a conceptual route for implementing small resonant antennas [7]–[17]. TL-MTM structures operating at resonance were first proposed in order to implement small printed antennas in [8] and [9]. Furthermore, a dual-band MTM-inspired small antenna for WiFi applications was shown in [18] and multiband MTM resonant antennas were shown to exhibit several left-handed modes in [19]. However, typically TL-MTM antennas suffer from narrow bandwidths. Recently, [12] addressed the bandwidth problem by proposing a two-arm TL-MTM antenna resonating at two closely spaced frequencies. Another method to enhance the bandwidth consists of merging two resonances together in a TL-MTM printed monopole antenna [20].

In this work, a compact tri-band monopole antenna is proposed using reactive loading, that was inspired by previous TL-MTM work, and a "defected" ground-plane [21], in order to meet the specifications of the WiFi bands (lower WiFi band of 2.40 GHz – 2.48 GHz and upper WiFi band of 5.15 GHz – 5.80 GHz) and the WiMAX (3.30 GHz – 3.80 GHz) band while maintaining a small form factor. Herein, we thoroughly explain the operation of the proposed tri-band antenna and we fully characterize its performance both numerically and experimentally. As shown in Fig. 1, the proposed co-planar waveguide (CPW)-fed monopole antenna is loaded in a left-handed manner, inspired by the NRI-TL metamaterial π unit cell [11].

Manuscript received June 18, 2009; revised September 25, 2009; accepted October 27, 2009. Date of publication January 26, 2010; date of current version April 07, 2010. The work of J. Zhu was supported by an IEEE Antenna and Propagation Society Graduate Fellowship.

The authors are with the Edward S. Rogers Sr. Department of Electrical and Computer Engineering, University of Toronto, Toronto, ON M5S 3G4, Canada (e-mail: jiangzhu@waves.utoronto.ca; gelefth@waves.utoronto.ca).

Color versions of one or more of the figures in this paper are available online at http://ieeexplore.ieee.org.

Digital Object Identifier 10.1109/TAP.2010.2041317

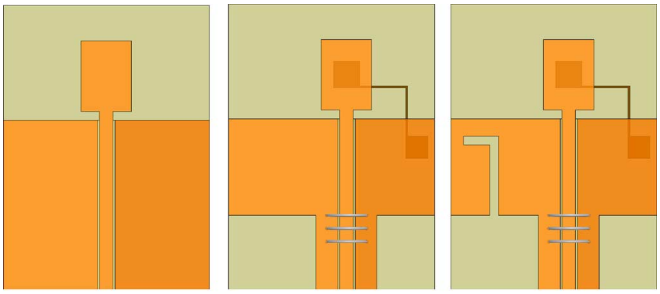

(a) (b) (c)

Fig. 2. (a) Case 1: unloaded monopole antenna, (b) Case 2: dual-band monopole antenna with single-cell MTM loading and (c) Final: tri-band monopole antenna with single-cell MTM loading and a "defected" ground. The dimensions of these antennas are given in the caption of Fig. 1. (a) Case 1. (b) Case 2. (c) Final.

This loading consists of a single MTM cell which allows the monopole antenna to operate in two modes [20], covering both the WiFi bands. The first is a folded monopole mode, where the monopole together with the single-cell MTM loading forms a folded monopole around the frequency of 5.5 GHz [11]; The second mode is a dipole mode where the single-cell MTM loading forces horizontal currents to flow along the top edges of the ground-plane, thus rendering the entire ground a radiator at around 2.5 GHz. It will be shown in Section II, that the currents corresponding to the two modes are orthogonal to each other, as shown in Fig. 5. The third resonance covering the WiMAX band from 3.3 GHz to 3.8 GHz, is achieved by "defecting" the ground-plane by cutting an L-shaped slot from one side of the CPW ground. Air bridges are added at the antenna terminals to ensure that only balanced currents flow on the CPW feedline. The resulting antenna is compact (including the ground-plane), completely uniplanar, low profile and "via-free". Therefore, the proposed antenna is easy to fabricate using simple photolithography. A prototype antenna has been fabricated and tested. The measurements show good impedance matching at the WiFi and WiMAX bands, orthogonal pattern diversity in each of the WiFi bands and a reasonable radiation efficiency, all of which make it well suited for wireless LAN applications.

II. Antenna Design

The antenna was designed on a low-cost FR4 substrate with height $h_{sub} = 1.59$ mm, $\varepsilon_r = 4.34$ and $\tan\delta = 0.016$. A rectangular patch was chosen as the monopole radiation element. The length of the patch was adjusted according to the general design guideline that the lowest resonance is determined when the length of the monopole, L_m, is approximately $\lambda_g/4$. Therefore, an $L_m = 8.0$ mm monopole results in the lowest resonance occurring at 6.0 GHz, as can be seen in Fig. 4. This refers to the initial design where the metamaterial-inspired reactive loading and the "defected" ground-plane are not employed, which is shown as Case 1 in Fig. 2. In order to compare the performances with the proposed tri-band antenna shown in Fig. 1, the size of the monopole element and the width of the ground for Case 1 were kept the same as the proposed design. However, the length of the ground in Case 1 was adjusted to 20 mm in order to achieve good impedance matching. The antenna was fed by a CPW transmission-line, which can be easily integrated

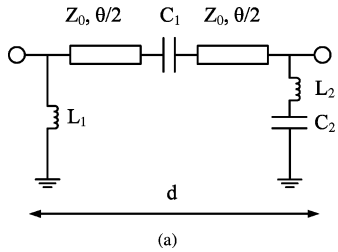

(a)

Fig. 3. The equivalent circuit when the proposed tri-band antenna operates at the monopole mode. The dimension d refers to the size of the NRI-TL unit cell and it corresponds to roughly the length of the monopole L_m with reference to Fig. 1(a).

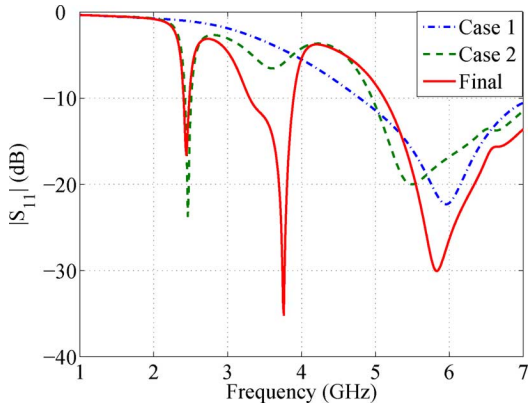

Fig. 4. Simulated $|S_{11}|$ for Case 1: unloaded monopole antenna, Case 2: dual-band monopole antenna with single-cell MTM loading and Final: tri-band monopole antenna with single-cell MTM loading and a "defected" ground, as shown in Fig. 2.

with other CPW-based microwave circuits printed on the same substrate. The CPW feed was connected to the coaxial cable through a standard 50 Ω SMA connector. All the structures were simulated in the finite-element method (FEM) based full-wave solver, Ansoft HFSS. The connector and coaxial cable were included in all simulations to characterize their effects on the antenna performance. Since the operating frequency of the initial design (unloaded monopole) was above the range of interest for existing wireless LAN applications, different approaches using single-cell MTM loading and a "defected" ground were pursued to create the corresponding second and third resonances, at a lower frequency range in order to meet the wireless LAN specifications.

A. Single-Cell Metamaterial Reactive Loading

In order to maintain the antenna's small form-factor while decreasing the operating frequency, the CPW monopole was loaded with a single asymmetric negative-refractive-index transmission-line (NRI-TL) metamaterial-based π unit cell. The equivalent circuit for the antenna of Fig. 1 is shown in Fig. 3 (at the folded monopole mode). The series capacitance, C_1, was formed between the monopole on the top of the substrate and the rectangular patch on the bottom of the substrate (see Fig. 1(b)). The MTM cell was asymmetrically loaded with two shunt inductances, L_1 and L_2. L_1 was formed by the inductive strip at the base of the monopole, while L_2 was formed by the thin inductive strip that joins the rectangular patch beneath

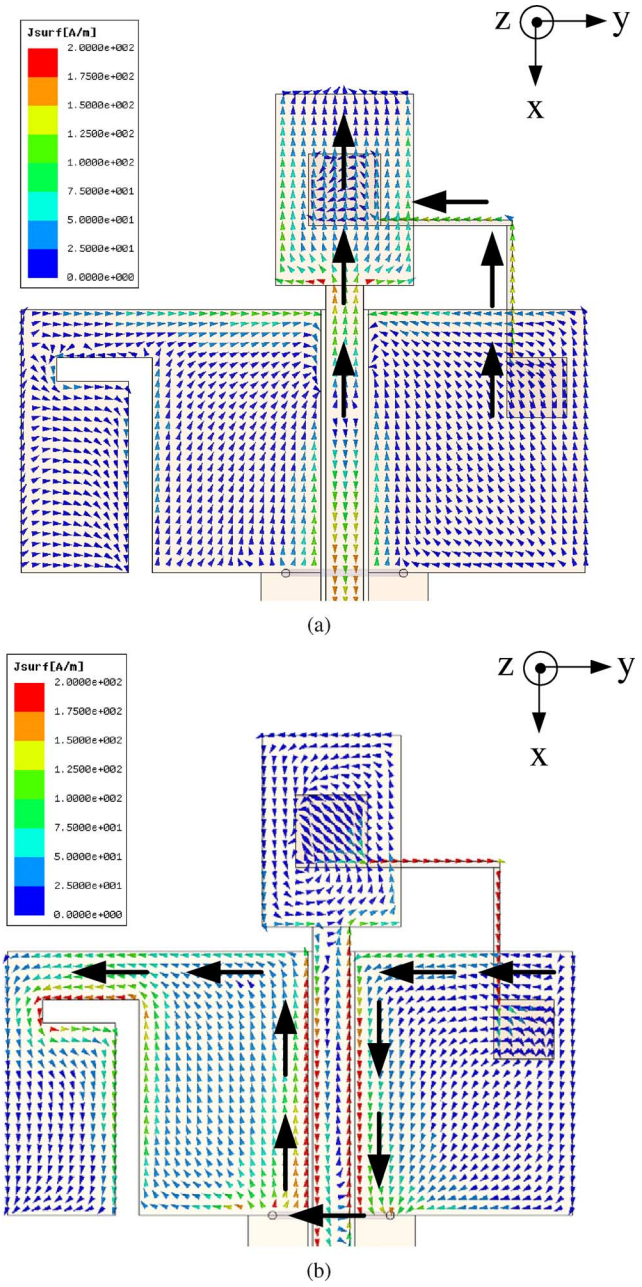

Fig. 5. HFSS-simulated surface current distribution on the conductors of the tri-band monopole antenna with single-cell MTM loading and a "defected" ground-plane at the resonant frequencies of (a) 5.80 GHz and (b) 2.44 GHz. (a) Folded monopole mode (5.80 GHz). (b) Dipole mode (2.44 GHz).

the monopole to the rectangular patch beneath the right-hand ground plane.

In order to simplify the fabrication, a via-free approach to implement the asymmetric π unit cell was used, which can be realized using low-cost thin-film technology. In order to achieve a shunt RF short to ground at high frequencies, the capacitor C_2 was used, which connects the shunt inductor L_2 to ground (see Fig. 1(b)). The capacitor C_2 was formed between the right-hand ground plane and the rectangular patch beneath it.

Case 2 in Fig. 2 refers to the dual-band monopole antenna with single-cell MTM loading. In Case 2, the feature of the

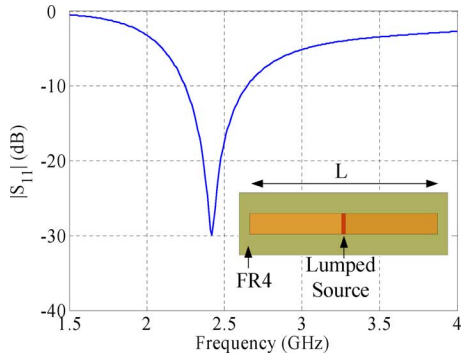

Fig. 6. Simulated $|S_{11}|$ of the equivalent dipole antenna representing the tri-band monopole antenna with single-cell MTM loading and a "defected" ground-plane when operating under the dipole mode, as shown in Fig. 5(b).

"defected" ground is temporarily removed, while the other geometrical parameters remain the same as the tri-band antenna shown in Fig. 1(a). From Fig. 4, it can be observed that the monopole antenna with this single unit-cell MTM loading exhibits dual-resonance characteristics [20]. The geometrical parameters, namely the size of the square patches underneath the monopole patch and the length of the thin strip determine C_1, C_2 and L_2 shown in Fig. 3, respectively. They were adjusted in order to obtain in-phase currents along the top monopole and along the thin bottom strip at the resonant frequency around 6.0 GHz. When operating in the folded monopole mode, the antenna acts as a two-arm folded monopole along the x-axis, similar to the four-arm folded monopole of [11]. As discussed in [11], it is possible to eliminate the odd-mode currents along the CPW feedline by adjusting the printed lumped elements, thus enabling the x-directed even-mode currents on the antenna to radiate. This can be seen from the HFSS-simulated current distribution of Fig. 5(a).

In addition to the monopole resonance at around 5.0 GHz – 6.0 GHz, the metamaterial loading introduces a second resonance around 2.4 GHz – 2.5 GHz, which is desired for WiFi applications. At this frequency, the antenna no longer acts as a folded monopole along the x-axis, but rather as a dipole oriented along the y-axis, as shown in Fig. 5(b), where the current path was sketched from HFSS. Since the currents along the right edge of the left ground-plane section are flowing against the currents along the left edge of the right ground-plane section, only the in-phase currents along the top edges of both the ground-plane sections contribute to the radiation, which renders the ground-plane as the main radiating element. The length of the current path $W_g + 2L_g$, which is related to the size of the ground-plane, determines the resonant frequency. This is verified by the simulation for a central-fed dipole shown in Fig. 6. In Fig. 6, the equivalent dipole was simulated with the same substrate and the same length of $L = W_g + 2L_g$. The resulting resonant frequency is 2.42 GHz, which agrees with the dipole-mode resonance for the simulated $|S_{11}|$ of the tri-band antenna shown in Fig. 4. Besides, since the dipole-mode currents for the proposed design are flowing in a meandered path, an even larger miniaturization factor is achieved, compared to the loaded monopole antenna reported in [20] where the dipole-mode currents only flow along the top edges of the ground-plane.

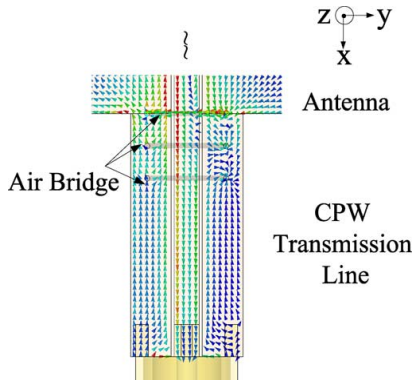

Fig. 7. HFSS-simulated current distribution at the intersection between the antenna terminal and the CPW feedline under the dipole mode of operation.

Ideally, the dipole mode would not be excited for the regular monopole antenna due to the symmetric current distribution along the central line of the CPW feedline. In order to excite this mode, a single unit cell of MTM reactive loading was utilized. At low frequencies, the host transmission-line sections are very short and can be considered negligible. Assuming that the feed is placed at the base of the shunt inductor L_1, the entire circuit is simply transformed into a series resonator formed between the loading capacitors C_1 and C_2 and the loading inductors L_1 and L_2, as shown in Fig. 1(b). If the resonant frequency of the series resonator is designed to overlap with the dipole mode resonance of the antenna, it forms a short circuit and therefore forces the in-phase currents along the y-axis flowing from one side of the ground to the other, through the path shown in Fig. 5(b). This enables the ground-plane to radiate in a dipolar fashion, which is orthogonal to the radiation at the higher frequencies. Bearing in mind the design considerations discussed above, the optimized loading patches have dimensions of $3.0 \times 3.0\ \mathrm{mm}^2$ and $2.5 \times 2.5\ \mathrm{mm}^2$, respectively, and the two sections of thin strips have the same length of 5.5 mm and width of 0.25 mm. In addition, the position of the central line of the CPW inner conductor is tuned and placed 1.7 mm off from the central symmetry line of the antenna, in order to obtain a good impedance match to 50 Ω, which in turn results in asymmetric ground-planes, as shown in Fig. 1(a).

Since the currents need a path from one ground to the other, an air bridge made of copper wires was placed at the intersection between the antenna terminal and the extended CPW feedline, in order to provide a shorting path. Additional air bridges were placed at the CPW feed side and parallel to the first air bridge, which ensure balanced currents and preserve the CPW mode. Fig. 7 shows the transition of the currents from unbalanced to balanced at the terminal, where one can observe that the majority of the unbalanced currents pass through the first air bridge but after the third air bridge, they are effectively suppressed. It is worth mentioning that in practice, the CPW feed with air bridges can be replaced with a conductor backed CPW with a ground-via fence which offers the additional advantage of lower EMI radiation.

Lastly, it can been seen that there is a small S_{11} dip around 3.6 GHz for Case 2 shown in Fig. 4. This corresponds to another resonant current path along the ground plane, which is nevertheless weakly excited. The length of this current path is approximately $L_g + W_g$, which can be verified using an equivalent dipole simulation, similar to that shown in Fig. 6.

The dual-mode operation due to the metamaterial loading is, indeed, verified by the HFSS simulation for Case 2 shown in Fig. 2(b). As seen in Fig. 4, the simulated magnitude of S_{11} for the monopole antenna with single-cell MTM reactive loading (the dashed line) has a desired higher resonance at around 5.48 GHz which is lower than 6.0 GHz for Case 1 and covers the bandwidth ($< -10\,\mathrm{dB}$) starting from 4.95 GHz to up to 7 GHz, while the lower resonance is centered at 2.46 GHz and has a bandwidth of 90 MHz.

B. The "Defected" Ground-Plane Antenna

In order to create the third resonance to meet the requirement for the WiMAX application (3.30 GHz – 3.80 GHz) in the responses of the monopole antenna with the proposed reactive loading (Case 2 in Fig. 2(b)), a slot was cut out of the antenna ground-plane, thus forming a defected ground-plane. Similar to [22], an L-shaped slot was chosen to achieve a longer effective slot length, without having to increase the size of the ground-plane. However, unlike having the slot cut at the top edge of the ground [22], the proposed design has the slot cut at the bottom edge, to avoid the discontinuity of the current along the top edge of the ground-plane, which contributes to the dipole-mode radiation. The width of the slot is $g = 1\ \mathrm{mm}$ while the vertical and horizontal length of the slot, L_{s1} and L_{s2}, were adjusted in order to achieve a good impedance match throughout the WiMAX band. This leads to the final design topology as shown in Fig. 2(c). It can be seen from Fig. 4 (solid line) that inserting the L-shaped slot provides the third resonance around 3.5 GHz for the WiMAX band, while the dual-mode operation for the WiFi bands at around 2.5 GHz and 6.0 GHz is preserved.

The resonance due to the slot can be explained by observing the surface current distribution on the conductors of the antenna, as shown in Fig. 8. As can be seen, there is a strong concentration of the currents along the L-shaped slot on the left ground-plane. The slot forces the current to wrap around it and thus creates an alternate path for the current on the left ground-plane, whose length is approximately $\lambda_g/2$ at its resonance. It is also noted from Fig. 8 that the L-shaped slot does not significantly affect the balanced CPW mode, since it is placed far enough away from the CPW. Even if there were a minimal amount of unbalanced current, it would be eliminated by the air bridges applied at the intersection between the antenna and the extended CPW feedline, as shown in Fig. 7.

Fig. 9 shows the simulated magnitude of S_{11} for a parametric study of the length of the horizontal slot L_{s2}. It can be observed that the horizontal cut has a large influence on exciting the slot mode. When $L_{s2} = 0$, which refers to the case that there is only a vertical slot cut from the bottom, the slot mode is barely excited, compared with the simulated S parameter characteristics in the case without a "defected" ground (Case 2) in Fig. 4. Moreover, it can be seen that the vertical slot cut from the bottom doesn't affect the folded monopole and dipole modes. As L_{s2} is gradually increased, a better impedance match is achieved over

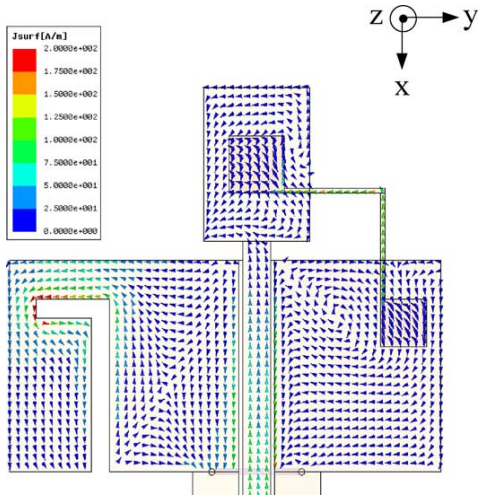

Fig. 8. HFSS-simulated surface current distribution on the conductors of the tri-band monopole antenna with single-cell MTM loading and a "defected" ground-plane at the resonant frequency of 3.76 GHz.

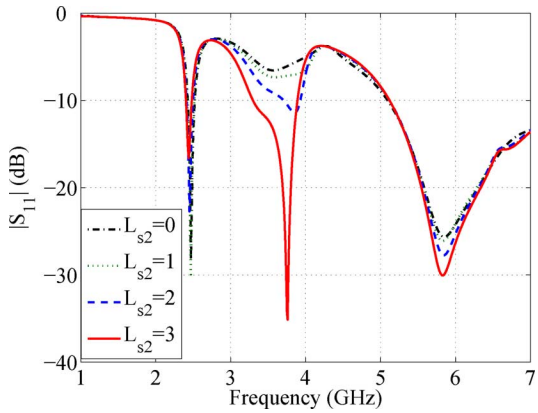

Fig. 9. Simulated $|S_{11}|$ of the tri-band monopole antenna with single-cell MTM loading and a "defected" ground-plane for the different lengths of the horizontal slot L_{s2}.

the WiMAX band, while the performances of the monopole and dipole modes are both preserved.

The final design of the tri-band monopole antenna with single-cell MTM reactive loading and a "defected" ground is shown in Fig. 1. The geometrical parameters were determined based on the previous discussion and were fine-tuned in order to meet the WiFi and WiMAX bands requirements. As shown in Fig. 1, the full size of the tri-band monopole antenna (including the ground-plane with the size of $L_g \times W_g = 11.0 \text{ mm} \times 23.5 \text{ mm}$) is 20.0 mm × 23.5 mm × 1.59 mm, or $\lambda_0/6.3 \times \lambda_0/5.3 \times \lambda_0/78.6$, with respect to the lowest resonant frequency of 2.45 GHz. The compact size and the tri-band performance of the antenna make it a good candidate for emerging WLAN applications.

III. Simulation and Experimental Results

The tri-band monopole antenna was fabricated and tested. The fabricated prototype is shown in Fig. 10, and the measured versus the simulated magnitude of S_{11} from HFSS are shown in Fig. 11. The antenna exhibits a simulated -10 dB bandwidth of 80 MHz for the lower WiFi band from 2.40 GHz to 2.48 GHz

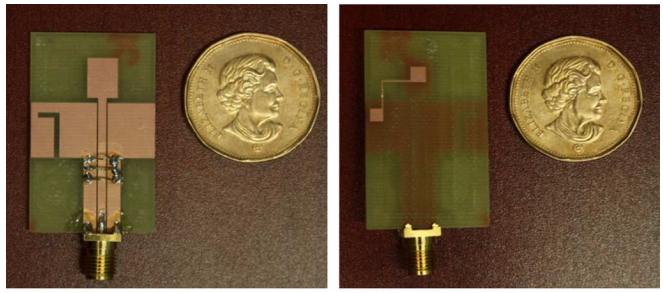

Fig. 10. The fabricated prototype of the tri-band monopole antenna with single-cell MTM loading and a "defected" ground-plane. (a) Front side. (b) Back side.

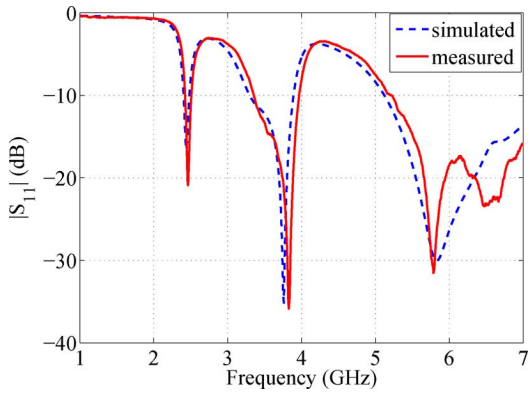

Fig. 11. Measured and HFSS simulated $|S_{11}|$ for the proposed tri-band monopole antenna with single-cell MTM loading and a "defected" ground.

and a bandwidth from 5.13 GHz to beyond 7 GHz for the higher WiFi band. It also exhibits a -10 dB bandwidth of 590 MHz for the WiMAX band from 3.30 GHz to 3.89 GHz. The performances beyond 7 GHz are out of the scope of our interest for WiFi and WiMAX applications. The measured -10 dB bandwidth is 90 MHz from 2.42 GHz to 2.51 GHz for the lower WiFi band, and from 5.20 GHz to beyond 7 GHz for the second WiFi band. The measured bandwidth for the WiMAX band is 620 MHz from 3.35 GHz to 3.97 GHz. The simulated results and the measured results show good agreement.

The simulated and measured radiation patterns for the proposed tri-band monopole antenna with single-cell MTM reactive loading and a "defected" ground-plane are plotted in Figs. 12–14 for the three principle planes at the frequencies of 5.50 GHz, 2.45 GHz and 3.50 GHz, respectively, where good agreement between the simulations and measurements can be observed. Fig. 12 shows the radiation patterns at 5.50 GHz for the E-plane (xz-plane and xy-plane) and the H-plane (yz-plane). The fact that the antenna exhibits radiation patterns with a horizontal x-directed linear E-field polarization, verifies that the antenna operates in a folded monopole mode around 5.50 GHz, due to the x-directed in-phase currents along the monopole and the thin vertical inductive strip, as shown in Fig. 5(a). The y-directed currents along the thin horizontal inductive strip have a contribution to the cross polarization in the xz-plane. It can also be seen that at this frequency, the slot on the left ground has a minimum contribution to the radiation since the currents are dominated by the x-directed

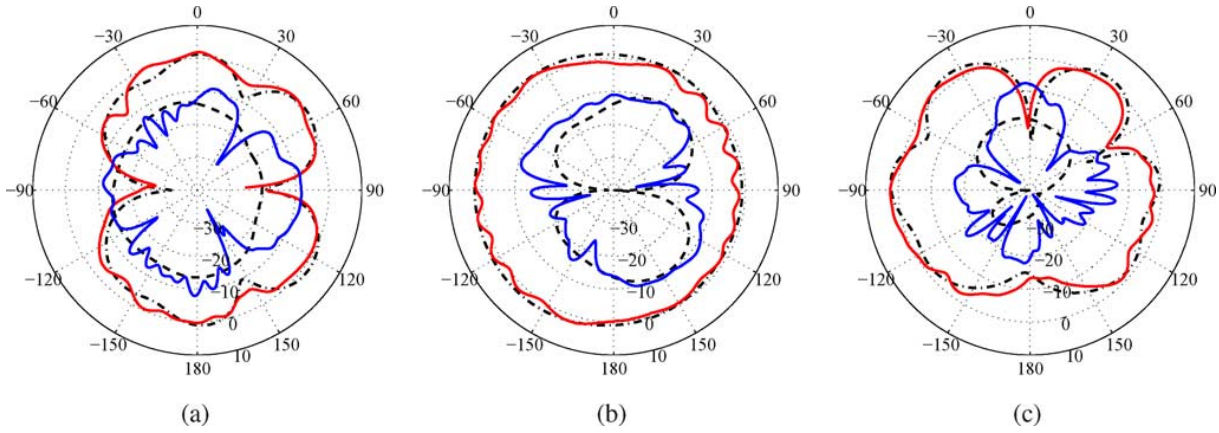

Fig. 12. Measured and simulated radiation patterns for the tri-band monopole antenna with single-cell MTM loading and a "defected" ground-plane at 5.50 GHz. Solid line: measured co-polarization, dashed black line: simulated co-polarization, solid blue line: measured cross-polarization, and dash-dot black line: simulated cross-polarization. (a) xz-plane. (b) yz-plane. (c) xy-plane.

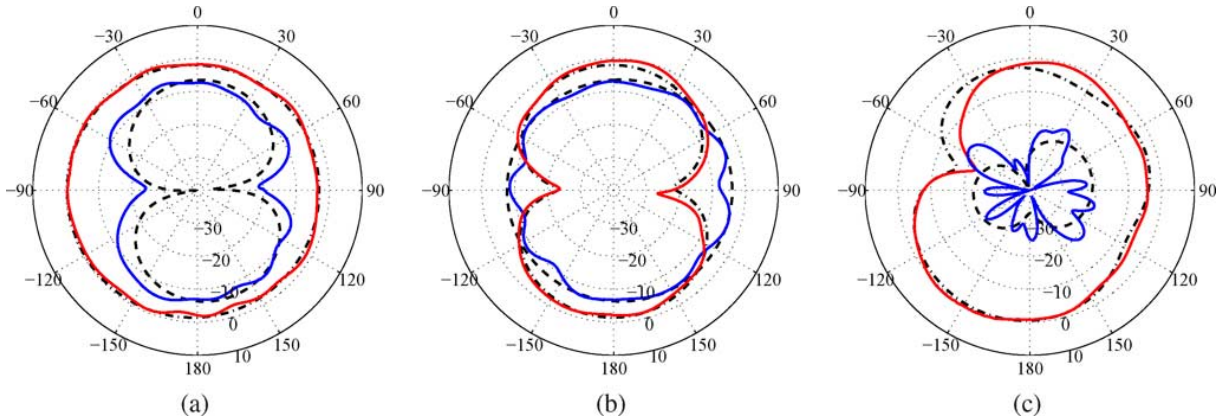

Fig. 13. Measured and simulated radiation patterns for the tri-band monopole antenna with single-cell MTM loading and a "defected" ground-plane at 2.45 GHz. Solid line: measured co-polarization, dashed black line: simulated co-polarization, solid blue line: measured cross-polarization, and dash-dot black line: simulated cross-polarization. (a) xz-plane. (b) yz-plane. (c) xy-plane.

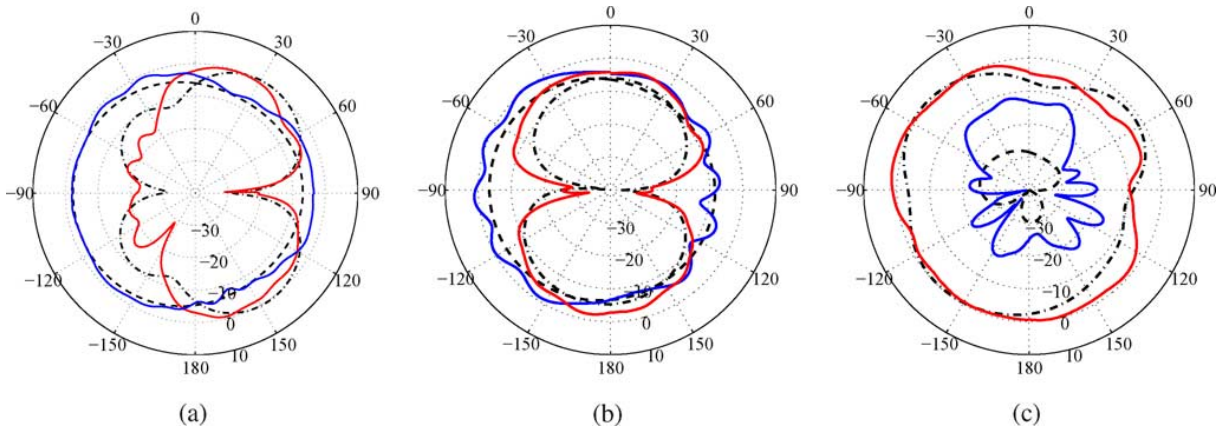

Fig. 14. Measured and simulated radiation patterns for the tri-band monopole antenna with single-cell MTM loading and a "defected" ground-plane at 3.50 GHz. Solid line: measured co-polarization, dashed black line: simulated co-polarization, solid blue line: measured cross-polarization, and dash-dot black line: simulated cross-polarization. (a) xz-plane. (b) yz-plane. (c) xy-plane.

ones along the monopole. At this frequency, the simulated radiation efficiency is 85.9%, which is in good agreement with the measured efficiency of 85.3%, using the Wheeler Cap method [23]. The Wheeler cap measurements were conducted according to the method described in [23], where the measured data in free-space and within the Wheeler cap were rotated on the Smith chart in order to obtain purely real values for the input resistance at resonance. The sphere used in the measurements is shown in Fig. 8 of [11], together with the pertinent details of its size. For this size Wheeler cap, its resonant frequency was

TABLE I
SIMULATED AND MEASURED GAIN AND RADIATION EFFICIENCY FOR THE TRI-BAND MONOPOLE ANTENNA WITH SINGLE-CELL MTM LOADING AND A "DEFECTED" GROUND-PLANE

Frequencies	Simulated Gain (HFSS)	Simulated Efficiency (HFSS)	Measured Gain	Measured Efficiency (Wheeler Cap Method)
2.45 GHz	0.98	69.8 %	1.14	67.4 %
3.50 GHz	1.25	80.8 %	1.15	86.3 %
5.50 GHz	2.05	85.9 %	1.78	85.3 %

calculated to be 0.69 GHz, which is well below the operating range of the tri-band antenna. Therefore, during the efficiency measurements at the three distinct resonant frequencies, special attention was paid in order to avoid any of the cavity resonances by slightly re-adjusting the position of the antenna within the Wheeler cap. Since the antenna was completely enclosed by the Wheeler-cap sphere during the measurements, this eliminated any potential radiation from the feed cable.

At 2.45 GHz, the y-directed currents contribute to the radiation, as shown in Fig. 5(b). This is consistent with the radiation patterns measured at the same frequency shown in Fig. 13. The radiation patterns in the xy-plane and the yz-plane, which correspond to the two E-planes of the ground-plane radiating mode, indicate that the structure radiates in a dipolar fashion at this frequency. Similar to [20], there is, however, a partial filling of the null around 90° in the xy-plane, that can be attributed to constructive interference from the x-directed currents along the CPW and the vertical thin inductive strip, and also the x-directed current around the slot on the left ground-plane. This additional current also manifests itself in the cross-polarization data of the yz-plane in the $\theta = 90^o$ direction, as can be seen in Fig. 13(b). In the xz-plane, which corresponds to the H-plane of the radiating ground-plane, the radiation pattern is as expected omnidirectional. Therefore, at 2.45 GHz, the antenna exhibits a y-directed linear E-field polarized radiation pattern. It is orthogonal to the one observed at 5.50 GHz, which verifies the in-phase y-directed currents across the ground. The simulated and measured efficiencies are 69.8% and 67.4%, respectively, which show good agreement.

Fig. 14 shows the radiation patterns at 3.50 GHz. Since the L-shaped slot which is cut out of the left ground-plane results in meandered currents along both the x-direction and the y-direction, which have independent contributions to the radiation, it is observed from Fig. 14 that the antenna exhibits two linear electric fields that are orthogonally polarized in both the x and y directions. Additionally, the axial ratio attains values close to, but greater than, one around the $\theta = 0°$ broadside direction, indicating circular polarization behavior. The measured efficiency at this frequency is 86.3%, compared to a simulated efficiency of 88.2% at the same frequency.

The measured and simulated gain and radiation efficiency values, at the frequencies of 2.45, 3.50, and 5.50 GHz, are summarized in Table I.

IV. CONCLUSION

A tri-band and compact monopole antenna is proposed, that can be used for WiFi and WiMAX applications. The antenna consists of a regular CPW-fed printed monopole antenna with the embedded features of metamaterial-based single-cell reactive loading and a "defected" ground-plane, which introduce another two resonances at the lower frequencies, in addition to the monopole resonance. The theoretical performance is verified by full-wave simulations and experimental data. The fabricated prototype with a size of $\lambda_o/6.3 \times \lambda_o/5.3 \times \lambda_o/78.6$ provides a 90 MHz (-10 dB) bandwidth from 2.42 GHz to 2.51 GHz for the IEEE 802.11b/g/n standard (lower WiFi band) and a broad band from 5.20 GHz to beyond 7 GHz for the IEEE 802.11a/n standard (upper WiFi band), and also a bandwidth of 620 MHz from 3.35 GHz to 3.97 GHz for the WiMAX band. The antenna exhibits dipole-like and monopole-like radiation patterns within the lower and upper WiFi bands, respectively, which are orthogonal to each other. The radiation patterns at the WiMAX band exhibit two orthogonal linear E-field polarizations as expected. Reasonable radiation efficiencies, in the range of 70% – 90%, are obtained for all three bands. Fed by the CPW transmission-line, the proposed antenna can be easily integrated with CPW-based microwave circuits. These attributes make the proposed antenna well suited for emerging wireless applications.

ACKNOWLEDGMENT

The authors would like to thank T.V. C.T. Chan at the University of Toronto for assisting in the measurement of the prototype antenna. Financial support from Intel corporation is gratefully acknowledged.

REFERENCES

[1] Y. Ge, K. Esselle, and T. Bird, "Compact triple-arm multiband monopole antenna," in *Proc. IEEE Int. Workshop on: Antenna Technology Small Antennas and Novel Metamaterials*, Mar. 2006, pp. 172–175.

[2] S. Yang, C. Zhang, H. K. Pan, A. E. Fathy, and V. K. Nair, "Frequency-reconfigurable antennas for multiradio wireless platforms," *IEEE Microw. Mag.*, vol. 10, no. 1, pp. 66–83, Feb. 2009.

[3] S. Yang, A. E. Fathy, S. El-Ghazaly, H. K. Pan, and V. K. Nair, "A novel hybrid reconfigurable multi-band antenna for universal wireless receivers," presented at the Electromagnetic Theory Symp., Jul. 2007.

[4] G. V. Eleftheriades, A. K. Iyer, and P. C. Kremer, "Planar negative refractive index media using periodically loaded transmission lines," *IEEE Trans. Microw. Theory Tech.*, vol. 50, no. 12, pp. 2702–2712, Dec. 2002.

[5] G. V. Eleftheriades and K. G. Balmain, *Negative-Refraction Metamaterials: Fundamental Principles and Applications*. Hoboken/Piscataway, NJ: Wiley/IEEE Press, 2005.

[6] C. Caloz and T. Itoh, "Novel microwave devices and structures based on the transmission-line approach of meta-materials," in *Proc. IEEE MTT-S Int. Microwave Symp.*, Jun. 2003, pp. 195–198.

[7] G. V. Eleftheriades, "Enabling RF/microwave devices using negative-refractive-index transmission-line (NRI-TL) metamaterials," *IEEE Antennas Propag. Mag.*, vol. 49, no. 2, pp. 34–51, Apr. 2007.

[8] G. V. Eleftheriades, A. Grbic, and M. Antoniades, "Negative-refractive-index transmission-line metamaterials and enabling electromagnetic applications," in *IEEE Antennas and Propagation Society Int. Symp. Digest*, Jun. 2004, pp. 1399–1402.

[9] A. Sanada, M. Kimura, H. Kubo, C. Caloz, and T. Itoh, "A planar zeroth order resonator antenna using a left-handed transmission line," in *Proc. 34th Eur. Microwave Conf. (EuMC)*, Amsterdam, The Netherlands, Oct. 2004, pp. 1341–1344.

[10] F. Qureshi, M. A. Antoniades, and G. V. Eleftheriades, "A compact and low-profile metamaterial ring antenna with vertical polarization," *IEEE Antennas Wireless Propag. Lett.*, vol. 4, pp. 333–336, 2005.
[11] M. A. Antoniades and G. V. Eleftheriades, "A folded-monopole model for electrically small NRI-TL metamaterial antennas," *IEEE Antennas Wireless Propag. Lett.*, vol. 7, pp. 425–428, 2008.
[12] J. Zhu and G. V. Eleftheriades, "A compact transmission-line metamaterial antenna with extended bandwidth," *IEEE Antennas Wireless Propag. Lett.*, vol. 8, pp. 295–298, 2009.
[13] R. W. Ziolkowski and A. Erentok, "Metamaterial-based efficient electrically small antennas," *IEEE Trans. Antennas Propag.*, vol. 54, pp. 2113–2130, Jul. 2006.
[14] A. Erentok and R. W. Ziolkowski, "Metamaterial-inspired efficient electrically small antennas," *IEEE Trans. Antennas Propag.*, vol. 56, pp. 691–707, Mar. 2008.
[15] R. W. Ziolkowski, "An efficient, electrically small antenna designed for VHF and UHF applications," *IEEE Antennas Wireless Propag. Lett.*, vol. 7, pp. 217–220, 2008.
[16] A. Lai, K. Leong, and T. Itoh, "Infinite wavelength resonant antennas with monopolar radiation pattern based on periodic structures," *IEEE Trans. Antennas Propag.*, vol. 55, pp. 868–876, Mar. 2007.
[17] J.-G. Lee and J.-H. Lee, "Zeroth order resonance loop antenna," *IEEE Trans. Antennas Propag.*, vol. 55, pp. 994–997, Mar. 2007.
[18] J. Zhu and G. V. Eleftheriades, "Dual-band metamaterial-inspired small monopole antenna for WiFi applications," *Electron. Lett.*, vol. 45, no. 22, pp. 1104–1106, Oct. 2009.
[19] C.-J. Lee, K. Leong, and T. Itoh, "Composite right/left-handed transmission line based compact resonant antennas for RF module integration," *IEEE Trans. Antennas Propag.*, vol. 54, pp. 2283–2291, Aug. 2006.
[20] M. A. Antoniades and G. V. Eleftheriades, "A broadband dual-mode monopole antenna using NRI-TL metamaterial loading," *IEEE Antennas Wireless Propag. Lett.*, vol. 8, pp. 258–261, 2009.
[21] J. Zhu, M. A. Antoniades, and G. V. Eleftheriades, "A tri-band compact metamaterial-loaded monopole antenna for WiFi and WiMAX applications," presented at the IEEE Antennas and Propagation Society Int. Symp., Jun. 2009.
[22] M. A. Antoniades and G. V. Eleftheriades, "A compact multi-band monopole antenna with a defected ground plane," *IEEE Antennas Wireless Propag. Lett.*, vol. 7, pp. 652–655, 2008.
[23] W. E. McKinzie, III, "A modified wheeler cap method for measuring antenna efficiency," in *Proc. IEEE Antennas and Propagation Society Int. Symp.*, Jul. 1997, pp. 542–545.

Jiang Zhu (S'06) received the B.Eng. degree in electrical engineering from Zhejiang University, Hangzhou, China, in 2003 and the M.A.Sc. degree in electrical engineering from McMaster University, Hamilton, ON, Canada, in 2006. He is currently working toward the Ph.D. degree at the University of Toronto, Toronto, ON, Canada.

In August 2003, he joined the Positioning and Wireless Technology Center, Nanyang Technological University, Singapore. From 2004 to 2006, he was a Research Assistant with the Computational Electromagnetics Research Laboratory and the Simulation Optimization Systems Research Laboratory, Department of Electrical and Computer Engineering, McMaster University. He joined the Electromagnetics Group, University of Toronto, in September 2006, where he is currently a Research Assistant and Teaching Assistant. His research interests are electromagnetic metamaterials, small antennas, microwave computer-aided design and microwave imaging.

Mr. Zhu is the recipient of IEEE Antenna and Propagation Society Doctoral Research Awards for 2008–2009 and the Chinese Government Award for Outstanding Self-Financed Student Abroad 2008.

Marco A. Antoniades (S'99–M'09) received the B.A.Sc. degree in electrical engineering from the University of Waterloo, ON, Canada, in 2001, and the M.A.Sc. and Ph.D. degrees in electrical engineering from the University of Toronto, ON, Canada, in 2003 and 2009, respectively.

From 1997 to 2001, he worked for various telecom/engineering companies, including Spacebridge, Cisco, Honeywell, Ericsson, The Cyprus Telecommunications Authority and Westinghouse, as part of the work-experience program at the University of Waterloo. From 2001 to 2009, he was a teaching assistant at the University of Toronto, where he contributed to the design and teaching of undergraduate courses relating to electromagnetics. During the same period, he was a research assistant at the University of Toronto, where he was involved in the development of microwave devices and antennas based on negative-refractive-index transmission-line (NRI-TL) metamaterials. Currently, he is a Postdoctoral Fellow at the University of Toronto, pursuing his research interests in antenna design and miniaturization, RF/microwave circuits and devices, periodic electromagnetic structures and negative-refractive-index metamaterials.

Dr. Antoniades was a recipient of the Edward S. Rogers Sr. Graduate Scholarship from the Department of Electrical and Computer Engineering at the University of Toronto for 2003/04 and 2004/05. He received the first prize in the Student Paper Competition at the 2006 IEEE Antennas and Propagation Society (AP-S) International Symposium in Albuquerque, NM. In 2009, he was the recipient of the Ontario Post-Doctoral Fellowship from the Ministry of Research and Innovation of Ontario.

George V. Eleftheriades (S'86–M'88–SM'02–F'06) received the Diploma in Electrical Engineering from the National Technical University of Athens, Greece in 1988 and the M.S.E.E. and Ph.D. degrees in electrical engineering from the University of Michigan, Ann Arbor, in 1989 and 1993, respectively.

From 1994 to 1997, he was with the Swiss Federal Institute of Technology in Lausanne. Currently, he is a Professor in the Department of Electrical and Computer Engineering, University of Toronto, where he holds a combined Canada Research Chair/Velma M. Rogers Graham Chair in Engineering. His research interests include transmission-line and other electromagnetic metamaterials, small antennas and components for wireless communications, plasmonic and nanoscale optical components and structures, fundamental electromagnetic theory and electromagnetic design of high-speed interconnects.

Prof. Eleftheriades received the Ontario Premier's Research Excellence Award in 2001 and an E.W.R. Steacie Fellowship from the Natural Sciences and Engineering Research Council of Canada in 2004. He served as an IEEE AP-S Distinguished Lecturer during the period 2004–2009. Amongst his other scholarly achievements he is the recipient of the 2008 IEEE Kiyo Tomiyasu Technical Field Award "for pioneering contributions to the science and technological applications of negative-refraction electromagnetic materials." He is an IEEE Fellow and has been elected a Fellow of the Royal Society of Canada in 2009. He serves as an elected member of the IEEE AP-S AdCom and as an Associate Editor of the IEEE TRANSACTIONS ON ANTENNAS AND PROPAGATION. He is a member of the Technical Coordination Committee MTT-15 (Microwave Field Theory). He is the general chair of the IEEE AP-S/URSI 2010 Int. Symposium to be held in Toronto Canada in July 2010.